Spin pumping and anisotropic magnetoresistance voltages in magnetic bilayers: Theory and experiment

A. Azevedo,[1,*] L. H. Vilela-Leão,[1] R. L. Rodríguez-Suárez,[2] A. F. Lacerda Santos,[1] and S. M. Rezende[1]

[1]*Departamento de Física, Universidade Federal de Pernambuco, Recife, Pernambuco 50670-901, Brazil*

[2]*Facultad de Física, Pontificia Universidad Católica de Chile, Casilla 306, Santiago, Chile*

(Received 6 June 2010; revised manuscript received 29 January 2011; published 4 April 2011)

We investigate experimentally and theoretically the dc voltage generated in ferromagnetic and nonmagnetic metal bilayers under ferromagnetic resonance. The voltage is given by a superposition of the contributions from spin pumping (V_{SP}) and anisotropic magnetoresistance (V_{AMR}). A theoretical model is presented that separately determines V_{SP} and V_{AMR} as a function of the applied static field intensity as well the in-plane angle. The model is used to interpret a detailed set of data obtained in a series of $Ni_{81}Fe_{19}$/Pt samples excited by in-plane ferromagnetic resonance. The results show excellent agreement between theory and the measured voltages as a function of the Permalloy and Pt layer thicknesses. Our findings show that the quantitative separation of both effects is crucial to the interpretation of experiments and the determination of the spin Hall angle and spin-diffusion length.

DOI: 10.1103/PhysRevB.83.144402 PACS number(s): 72.25.Pn, 72.25.Mk, 72.25.Rb, 75.76.+j

I. INTRODUCTION

The unique properties of spin-polarized transport in magnetic nanostructures has led to the discovery of several fascinating phenomena in recent years, ranging from the giant magnetoresistance in metallic multilayers to current driven magnetization dynamics in nanostructures.[1] The latter effect has received considerable attention recently and, currently, there is a wealth of experimental data on the dc current excitation of the magnetization precession with microwave frequency and sound theoretical models for their interpretation.[2–7] A phenomenon, which in some aspects is the inverse of this effect, is the generation of a dc voltage by microwave spin pumping. As proposed by Brataas *et al.*, a few years ago,[8,9] spin pumping occurs when a pure-spin current is injected into a normal metal (NM) thin layer by an adjacent ferromagnetic metal (FM) layer undergoing ferromagnetic resonance (FMR). The precessing spins act as a peristaltic pump, adiabatically injecting spins out of the FM layer into the adjacent NM layer without charge transport. The spin current through the NM layer generates a charge current along the layer by means of the inverse spin Hall effect (ISHE).[10]

The detection of a dc voltage in magnetic multilayers and single films under FMR has recently been reported by several groups.[10–20] However, in all previous papers, the data were interpreted by theoretical models that leave several unresolved questions regarding the detailed origin of the voltage generation mechanisms. One of the main problems arises from the fact that the measured dc voltage is the superposition of the spin-pumping dc voltage (V_{SP}) and the anisotropic magnetoresistance voltage (V_{AMR}). Thus, in order to obtain precise values for V_{SP}, one must have a correct theoretical model for V_{AMR}, in particular, regarding its symmetry properties with respect to the applied static magnetic field intensity H and the in-plane field angle. For example, in Ref. 15, the rf current induced in the FM layer is assumed to be 90° out of phase with the rf magnetization. This leads to a V_{AMR} that has only an antisymmetric component in field scan, so the values of V_{SP} extracted from the data are inaccurate.

In this paper, we describe an investigation of dc voltage generated by FMR and show unequivocally that the V_{AMR} has both symmetric and antisymmetric components in field scan, whereas V_{SP} has only a symmetric component. We also show that in our experimental arrangement V_{AMR} and V_{SP} have different symmetries with respect to the in-plane field angle. These two facts allow a precise separation between V_{AMR} and V_{SP} from the measured dc voltage. The theoretical model is used to interpret detailed data for a series of Py(t_{FM})/Pt(t_{NM}) bilayers and leads to excellent fits of theory to the measured spin-pumping voltage as a function of the NM and FM layer thicknesses. The quantitative separation of V_{SP} and V_{AMR} as a function of both t_{FM} and t_{NM} is fundamental in order to determine physical parameters such as spin Hall angle and spin-diffusion length.

II. EXPERIMENT AND MODEL

Direct-current voltages, generated by FMR in FM metal films and semiconductors, were investigated in the 1960s and 1970s.[21,22] In those early experiments, the samples were under the action of both electric and magnetic fields of microwave radiation. In our experiments, the sample is placed inside a microwave cavity in a nodal position of minimum rf electric field and maximum rf magnetic field. This precaution minimizes the generation of electric current by the rf electric field. The samples are bilayers of Py(t_{FM})/NM(t_{NM}), where NM = Cu, Ag, Pd, and Pt, with thicknesses t_{FM} and t_{NM} in the range of 1.7 to 40 nm deposited by magnetron sputtering on Si substrate slabs with lateral dimensions 1.5 × 3.0 mm. By using a shadow mask, the Py layer covers only the central part of the NM layer surface, thus Ag electrodes can be attached to the edges of the NM layer [Fig. 1(a)]. The samples, with two Cu electrodes attached with silver paint, are introduced through a small hole in the back wall of a rectangular microwave cavity tuned in the TE_{102} mode at 8.6 GHz. With this configuration, we can investigate the angular dependence of both the FMR excited in the Py layer, and the dc voltage [$V(H)$] that develops along the NM layer. As shown in Fig. 1(b), the reference frame x'-z' is fixed relative to the sample. In order to measure the angular dependence of dc voltage, the sample is rotated in the film plane varying the angle ϕ_0 with respect to the laboratory

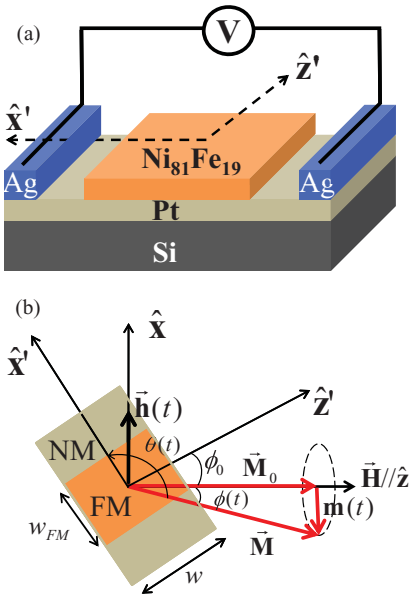

FIG. 1. (Color online) (a) Sketch showing the Py/Pt bilayer and the electrodes used to measure the dc voltage in the Pt layer along the x' axis. (b) Reference frames utilized to define the equations as described in the text. The angle ϕ_0 changes as the sample is rotated around the axis perpendicular to the plane of the sample.

frame of reference and $V(H)$ is measured along the $\hat{x}'$ direction. While the static field H points in the $\hat{z}$ direction the rf magnetic field is maintained along the $\hat{x}$ direction.

The main experimental observations are as follows: (i) $V(H)$ appears when the field value is near the resonance value H_r, given by the FMR equation for a film in-plane magnetized $\omega = \gamma H_r^{1/2}(H_r + 4\pi M_{\rm eff})^{1/2}$, where ω is the microwave frequency, γ is the gyromagnetic ratio, and $4\pi M_{\rm eff}$ is the effective magnetization of the Py film (H_r is large enough in order to saturate the magnetization along the film plane). (ii) The voltage increases with the atomic number Z of the normal metal with an approximately mZ^2 dependence, so it is larger for Pt. This is why we focus on Py/Pt bilayers. (iii) As shown in Fig. 2, the line shape of $V(H)$ varies strongly with the angle ϕ_0 between the field $\vec{H}$ and the sample axis z'. Depending on the angle, the line shape is a superposition of absorptive and dispersive curves, as observed by several authors.[10,11,15,18] (iv) For a fixed in-plane angle, the amplitude of V exhibits a linear dependence on the microwave incident power $P_{\rm rf}$. (v) The amplitude and shape of $V(H)$ also vary with the thicknesses $t_{\rm FM}$ and $t_{\rm NM}$. The variation of the line shape of $V(H)$ with the angle ϕ_0 is a result of the fact that it is given by the sum of the two contributions, anisotropic magnetoresistance $V_{\rm AMR}$ and spin pumping $V_{\rm SP}$. These contributions have different symmetries with respect to H, as shown in Ref. 15, and in our experiment, also with respect to the angle ϕ_0. The fit of

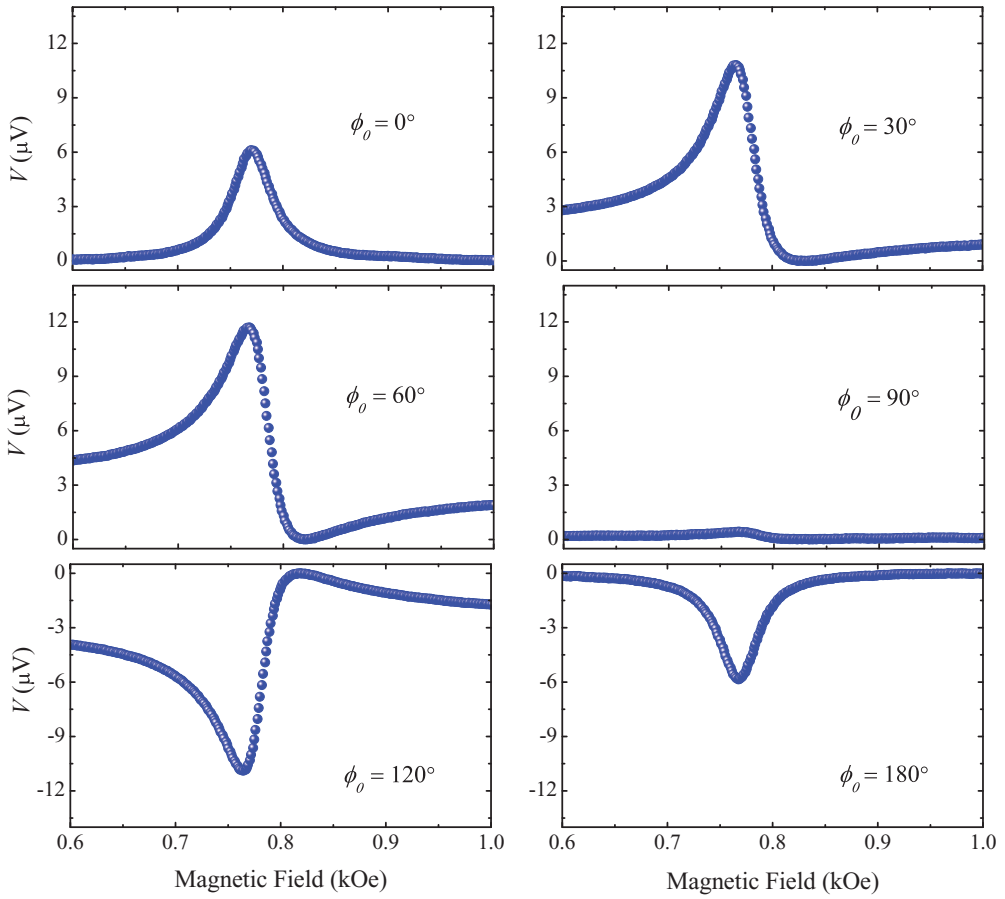

FIG. 2. (Color online) Field scans dc voltage measured in Py(18.5 nm)/Pt(6.0 nm) for several values of the angle ϕ_0 between the field $\vec{H}$ and the sample axis x'. For $\phi_0 = 0°$ and 180°, the voltage is only due to the spin-pumping contribution.

the theoretical models for $V_{\rm AMR}(H,\phi_0)$ and $V_{\rm SP}(H,\phi_0)$ to data allows a very accurate determination of the two contributions.

The origin of $V_{\rm AMR}(H,\varphi_0)$ is actually the classical induction effect due to the in-plane microwave magnetic field $\hat{x}\, h_{\rm rf}(t)$. Assume $\vec{M} = \hat{z}M_0 + \vec{m}(t)$, where M_0 is the equilibrium magnetization and $\vec{m}(t)$ is the rf transverse component rotating with frequency ω with an elliptical trajectory due to the strong demagnetization field. The classical induced current $I(t) = I_1\cos(\omega t)$, transverse to $\vec{h}_{\rm rf}(t)$, flowing through the FM layer produces the AMR voltage given by $V_{\rm AMR}(t) = (R_0 + R_A\cos^2\theta(t))\,(I(t)\sin\phi_0)$. Here the term $\sin\phi_0$ was introduced to take into account the component of $I(t)$ along the measurement direction $\hat{x}'$, $\theta(t)$ is the angle between the local magnetization and the $\hat{x}'$ axis, and $\phi(t)$ is the in-plane oscillation angle between magnetization and $\vec{H}$, as illustrated in Fig. 1(b). This is essential to obtain the dependence of AMR on the in-plane angle observed in the experiments. We assume that $\phi(t) = \phi_1\cos(\omega t + \varphi)$, where ϕ_1 is the maximum in-plane angle between the magnetization $\vec{M}$ and the field $\vec{H}$, and φ is the phase angle between the rf magnetization and the rf current, which is a function of H. By expanding the term $\cos^2\theta(t)$ and observing that $\theta(t) \cong \pi/2 + \phi_0 + \phi(t)$and the magnetization precession angle is very small, we obtain

$$V_{\rm AMR}(t) \cong [R_0 + R_A\sin^2\phi_0 + R_A\phi_1\sin(2\phi_0)\cos(\omega t + \varphi)] \times I_1\cos(\omega t)\sin\phi_0. \quad (1)$$

By taking the time average of $V_{\rm AMR}(t)$, we obtain

$$\langle V(t)\rangle = (1/2)I_1R_A\phi_1\ \sin 2\phi_0\sin\phi_0\cos\varphi. \quad (2)$$

By using $\phi_1 \approx |m_x|/M_0$ and expressing m_x in terms of h_x with the known equations for the Polder susceptibility tensor,[12,23] one can show that

$$V_{\rm AMR}(H,\phi_0) = \frac{R_AI_1A_{\rm xx}h_{\rm rf}}{2M_0}\left[\frac{\Delta {\rm H}^2\cos\varphi_{\rm I}}{({\rm H}-{\rm H_r})^2+\Delta {\rm H}^2} - \frac{({\rm H}-{\rm H_r})\Delta {\rm H}\sin\varphi_{\rm I}}{({\rm H}-{\rm H_r})^2+\Delta {\rm H}^2}\right]\sin 2\phi_0\ \sin\phi_0, \quad (3)$$

where $A_{xx} = [\gamma M_0(H_r + 4\pi M_{\rm eff})/\gamma\Delta H(2H_r + 4\pi M_{\rm eff})]$, ΔH is the half-FMR linewidth related to the Gilbert damping parameter α by $\Delta H = \alpha\omega/\gamma$, and φ_I is the phase between the rf current and the rf magnetization at the FMR condition $H = H_r$. Although the phase angle φ_I is a key parameter, it is not easy to be directly measured as was shown by Guan *et al.*[24] Equation (3) shows that $V_{\rm AMR}$ has two terms, one symmetric and another antisymmetric, with respect to the resonance field H_r. The amplitudes of the two terms depend on the phase angle φ_I and, only if it is 90°, will the contribution $V_{\rm AMR}(H)$ be antisymmetric relative to H_r. Most importantly, with the experimental arrangement in which $\hat{x}h_{\rm rf}$ is in the film plane and rotates with the static field, $V_{\rm AMR}(H,\phi_0)$ varies with angle ϕ_0 as $\sin(2\phi_0)\cdot\sin(\phi_0)$ which, as will be shown, is an angle dependence different from that of $V_{\rm SP}(H,\phi_0)$. As $I_1 \propto h_{\rm rf}$, the AMR contribution to the dc voltage is proportional to the microwave power. It is also important to remember that, as the out-of-plane magnetization component is small, the anomalous Hall effect contribution to the dc voltage is negligible.

The spin-pumping voltage has its origin in two combined processes, the spin-pumping mechanism proposed by Brataas, Tserkovnyak, and co-workers,[8,9] and the ISHE identified by Saitoh *et al.*[10] In Refs. 8 and 9, it is shown that a precessing magnetization in a FM layer injects a pure spin-current density into the adjacent NM layer, given by $\vec{J}_S(y) = \vec{J}_S(0)\{\sinh[(t_N - y)/\lambda_{\rm SD}]/\sinh(t_N/\lambda_{\rm SD})\}$. Due to the spin diffusion and relaxation, it decays through the NM layer with a spin-diffusion length $\lambda_{\rm SD}$. The spin-current density at the FM/NM interface ($y = 0$) is given by $\vec{J}_S(0) = (\hbar\tilde{A}_r/4\pi)(\hat{m}\times d\hat{m}/dt)$, where $\hat{m} = \vec{m}(t)/M_0$ and $\tilde{A}_r$ is the real part of the spin-pumping conductance.[8,9] It has been shown that, due to the spin-orbit interaction, the pure-spin current $\vec{I}_S$ gives rise to a charge current $\vec{I}_c$, a phenomenon identified as ISHE.[10] The charge current is transverse to $\vec{I}_S$ and is given by $\vec{I}_c = \gamma_H(e/\hbar)\vec{I}_S\times\vec{\sigma}$, where γ_H is a dimensionless coefficient representing the ISHE efficiency (named as the Hall angle), $\vec{\sigma}$ is the spin polarization, and e is the electron charge. Note that I_S and I_c have dimensions of torque and charge/time, respectively. The electric current I_c flowing along the NM layer produces a voltage along $\hat{x}'$ given by I_cR, where R is the resistance of the layer between the two electrodes. Integrating the current density through the cross section of the NM layer by using $V_{\rm SP} = R_{x'}\int(\langle\vec{J}_C(y,t)\rangle\cdot\hat{x}')\,da'$, one obtains the dc component of the spin-pumping voltage

$$V_{\rm SP}(H,\phi_0) = \frac{\gamma_H\lambda_{\rm SD}}{\sigma_N}\left(\frac{e\omega}{4\pi}\right)\frac{\tilde{A}_r}{t_{\rm NM}w}{\rm Im}\left(\frac{m_x^*m_y}{M_0^2}\right) \times\ \tanh(t_{\rm NM}/2\lambda_{\rm SD})\cos\phi_0, \quad (4)$$

where w and σ_N are, respectively, the width and the conductivity of the NM layer. Using the Polder tensor[23] to express m_x^* and m_y in terms of $h_{\rm rf}$ and using $\tilde{A}_r = 4\pi M_0V_{\rm FM}\alpha'/\gamma\hbar$ (Ref. 8), where $V_{\rm FM} = t_{\rm FM}w_{\rm FM}w$ is the volume of the FM layer and α' is the additional damping caused by the spin pumping,[8,25–27] one obtains

$$V_{\rm SP}(H,\phi_0) = -\frac{e\omega\gamma_H\lambda_{\rm SD}\alpha'}{\gamma\hbar M_0\sigma_N}\left[\frac{t_{\rm FM}w_{\rm FM}\tanh(t_{\rm NM}/2\lambda_{\rm SD})}{t_{\rm NM}}\right] \times A_{xx}A_{xy}\left[\frac{\Delta H^2}{(H-H_r)^2+\Delta H^2}\right]h_{\rm rf}^2\cos\phi_0, \quad (5)$$

where $A_{\rm xx}$ was defined in Eq. (3) and $A_{\rm xy} = \omega M_0/(2H_r + 4\pi M_{\rm eff})\gamma\Delta H$.

The dependence of the spin-pumping voltage on the thicknesses of the NM and FM layers is not as simple as it appears in the first bracket of Eq. (3) because, for small $t_{\rm FM}$, the damping is strongly dependent on the thicknesses. As is well known,[8,25–27] the Gilbert damping parameter can be written as $\alpha = \alpha_0 + \alpha'$, where α_0 is the intrinsic contribution and α' is the additional damping due to spin pumping given by[8]

$$\alpha' = \frac{\gamma\hbar g^{\uparrow\downarrow}}{4\pi M_0}\frac{1}{[1+(2\sqrt{\varepsilon/3}\coth(t_{\rm NM}/\lambda_{\rm SD}))^{-1}]}\frac{1}{t_{\rm FM}}. \quad (6)$$

Here $g^{\uparrow\downarrow}$ is the interface spin-mixing conductance (in units of e^2/h) and $\varepsilon = \tau_{\rm el}/\tau_{\rm sf}$ is the ratio of the spin-conserved to spin-flip relaxation times. Using Eq. (4) and the expressions for $A_{\rm xx}$ and $A_{\rm xy}$, one obtains an equation for $V_{\rm SP}(H,\varphi)$ with a

full dependence on the dimensions of the FM and NM layers, as well as on various physical parameters,

$$V_{\rm SP}(H,\phi_0) = -\frac{e\gamma_H\lambda_{\rm SD}h_{\rm rf}^2 w_{\rm FM}\gamma}{\sigma_N}\frac{g^{\uparrow\downarrow}}{4\pi} \times\left[\frac{1}{t_{\rm NM}}\frac{\tanh(t_{\rm NM}/2\lambda_{\rm SD})}{[1+(2\sqrt{\varepsilon/3}\tanh(t_{\rm NM}/\lambda_{\rm SD}))^{-1}]}\right] \times\left[\frac{1}{\alpha^2}\frac{(H_r+4\pi M_{\rm eff})}{(2H_r+4\pi M_{\rm eff})^2}\right] \times\frac{\Delta H^2}{(H-H_r)^2+\Delta H^2}\cos\phi_0. \quad (7)$$

III. RESULTS AND DISCUSSION

Equations (3) and (7) show clearly the most relevant features of $V_{\rm AMR}(H,\phi_0)$ and $V_{\rm SP}(H,\phi_0)$: (i) Both contributions exhibit a linear dependence on the incident microwave power (proportional to $h_{\rm rf}^2$), as observed in Ref. 11 and also confirmed in this work. (ii) For a fixed in-plane angle ϕ_0, $V_{\rm AMR}(H,\phi_0)$ has two components, one antisymmetric relative to H_r and another symmetric one, whereas $V_{\rm SP}(H,\phi_0)$ has only a symmetric component. (iii) Most importantly, $V_{\rm AMR}(H,\phi_0)$ and $V_{\rm SP}(H,\phi_0)$ have different dependences on the in-plane magnetic-field angle ϕ_0. This feature allows us to obtain accurate values for the three components of the dc voltage from the data for $V(H,\phi_0) = V_{\rm AMR}(H,\phi_0) + V_{\rm SP}(H,\phi_0)$. (iv) The dependence of $V_{\rm SP}(H,\phi_0)$ on the thickness of the FM layer is determined by the behavior of α and $4\pi M_{\rm eff}$, as discussed below.

In order to test the theoretical predictions of our model, we have done systematic measurements of $V(H)$ as a function of ϕ_0 in two series of Py($t_{\rm Py}$)/Pt($t_{\rm Pt}$) bilayers, one with fixed $t_{\rm NM} = 10.2$ nm and varying $t_{\rm FM}$ in the range 6–40 nm and another one with fixed $t_{\rm FM} = 18.5$ nm and varying $t_{\rm NM}$ in the range 2–40 nm. For each sample, the dc voltage was measured in steps of 10° for the in-plane angle ϕ_0. As shown in Fig. 2, the symmetry of $V(H)$ changes drastically with the angle ϕ_0. For $\phi_0 = 0$, 180°, $V(H)$ is perfectly symmetric relative to H_r because the only contribution to the dc voltage arises from $V_{\rm SP}$. On the other hand, $V(H)$ is asymmetric at any other angle because $V_{\rm AMR}$ has both symmetric and antisymmetric components. In order to extract the three components of the dc voltage from data, we write

$$V(H,\phi_0) = \left[V_{\rm AMR}^{\rm Sym}L(H) + V_{\rm AMR}^{\rm Antisym}L'(H)\right]\sin 2\phi_0\sin\phi_0 + V_{\rm SP}L(H)\cos\phi_0, \quad (8)$$

where $L(H) = \Delta H^2/[(H-H_r)^2+\Delta H^2]$ is the symmetric Lorentzian function, $L'(H) = \Delta H(H-H_r)/[(H-H_r)^2+\Delta H^2]$ is an antisymmetric function, and the three coefficients $V_{\rm AMR}^{\rm Sym}, V_{\rm AMR}^{\rm Antisym}$ and $V_{\rm SP}$ are the prefactors of Eqs. (3) and (7). Note that $V_{\rm AMR}^{\rm Antisym}/V_{\rm AMR}^{\rm Sym} = -\tan\phi_I$. Equation (8) can be written as $V(H,\phi_0) = A_{\rm Sym}(H,\phi_0) + B_{\rm Antisym}(H,\phi_0)$, so for each angle ϕ_0, we can obtain the symmetric and antisymmetric contributions. This is illustrated in Fig. 3 for a fixed $\phi_0 = 30°$, where the measured line shape (open circles) is adjusted to a symmetric (red line) plus an antisymmetric function (blue line). Figures 4(a) and 4(b) show the data for the angular dependence of $A_{\rm Sym}$ and $B_{\rm Antisym}$ obtained for

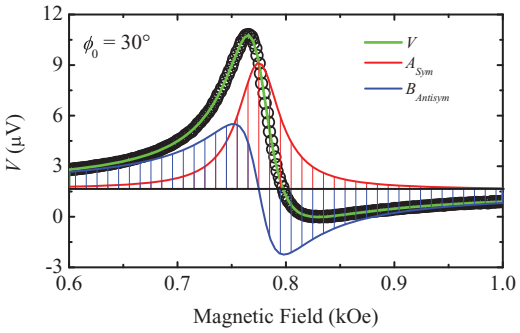

FIG. 3. (Color online) Measured dc voltage (open circles) obtained for Py(18.5 nm)/Pt(6.0 nm) at $\phi_0 = 30°$. The asymmetric green line is given by a superposition of symmetric (red line) and antisymmetric (blue line) components.

Py(18.5 nm)/Pt(6 nm) and theoretical fits made with the following equations:

$$A_{\rm Sym}(H,\phi_0) = \left(V_{\rm AMR}^{\rm Sym}\sin 2\phi_0\sin\phi_0 + V_{\rm SP}\cos\phi_0\right)L(H) \quad (9)$$

and

$$B_{\rm Antisym}(H,\phi_0) = V_{\rm AMR}^{\rm Antisym}\sin 2\phi_0\sin\phi_0 L'(H). \quad (10)$$

By fitting the data to the equations (9) and (10), one can obtain precise values for the three coefficients that determine the contributions of $V_{\rm AMR}(H,\phi_0)$ and $V_{\rm SP}(H,\phi_0)$ to $V(H,\phi_0)$. Using a microwave radiation with frequency 8.6 GHz and power of 58 mW, corresponding to $h_{\rm rf} \approx 0.35$ Oe in the back wall of a rectangular cavity with Q = 2500, the coefficients obtained for two bilayers of Py(18.5 nm)/Pt($t_{\rm NM}$) were $V_{\rm AMR}^{\rm Sym} = 4.4\ \mu$V, $V_{\rm AMR}^{\rm Antisym} = -1.6\ \mu$V, and $V_{\rm SP} = 5.2\ \mu$V for $t_{\rm NM} = 8$ nm; and $V_{\rm AMR}^{\rm Sym} = 5.0\ \mu$V, $V_{\rm AMR}^{\rm Antisym} = -3.1\ \mu$V, and

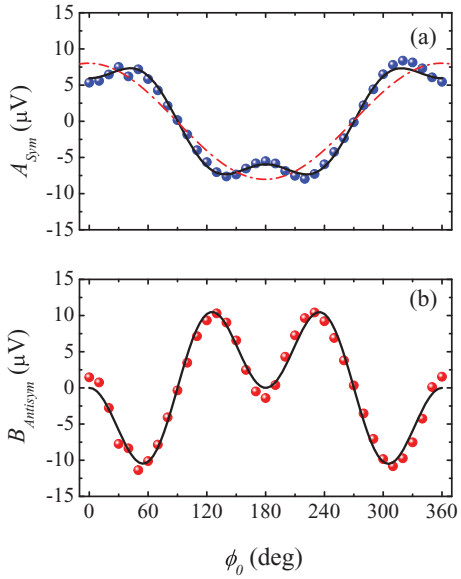

FIG. 4. (Color online) Angular dependence of data (symbols) and theoretical fits (lines) for the (a) symmetric and (b) antisymmetric $A_{\rm Sym}$ and $B_{\rm Antisym}$ components of the dc voltage obtained for Py(18.5 nm)/Pt(6.0 nm). The red dashed line in (a) shows the best fit assuming $V_{\rm AMR}^{\rm Sym} = 0$, as explained in the text.

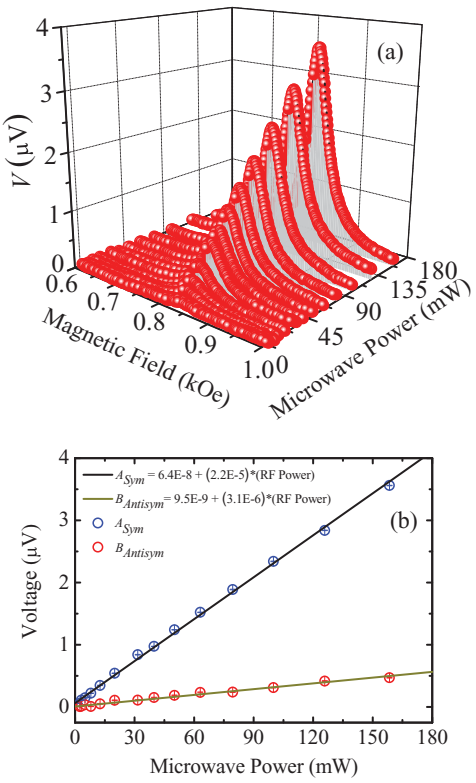

FIG. 5. (Color online) (a) Dependence of the dc voltage line shapes as a function of the incident microwave power for Py(18.5 nm)/Pt(6.0 nm) at $\phi_0 \cong 0°$. (b) Dependence of the symmetric and antisymmetric $A_{\rm Sym}$ and $B_{\rm Antisym}$ components of the dc voltage as a function of microwave incident power. The solid lines are linear fits to the data.

$V_{\rm SP} = 4.5\ \mu$V for $t_{\rm NM} = 16$ nm. From these values, we find $\varphi_I = 20.08°$ and $31.88°$ for $t_{\rm NM} = 8$ and 16 nm, respectively, which demonstrate that the phase between the rf current and the magnetization is quite different from the value of 90° assumed in Ref. 15. The dashed red line of Fig. 4(a) shows the best fit of the theory to data obtained by assuming $V_{\rm AMR}^{\rm Sym} = 0$. The poor fit demonstrates clearly that the symmetric component

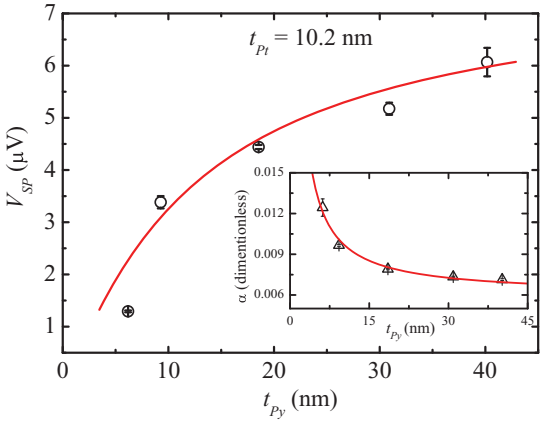

FIG. 6. (Color online) Data (symbols) and theoretical fit (line) for the spin-pumping voltage obtained in Py($t_{\rm FM}$)/Pt(10.2 nm) varying $t_{\rm FM}$ from 6 to 40 nm. Inset shows the dependence of the Gilbert damping parameter as a function of the FM layer thickness.

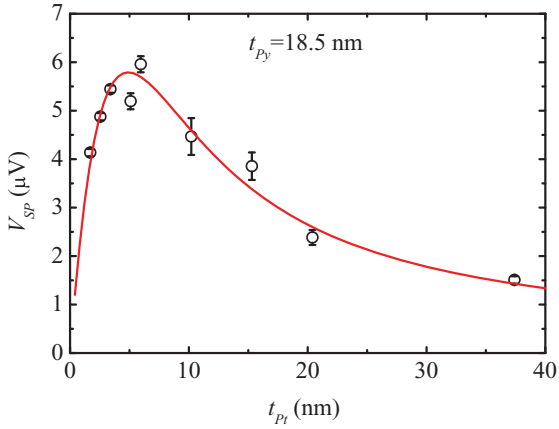

FIG. 7. (Color online) Data (symbols) and theoretical fit (line) for the spin-pumping voltage obtained in Py(18.5 nm)/Pt($t_{\rm NM}$) varying $t_{\rm NM}$ from 1.7 to 37 nm.

of the AMR voltage can not be assumed to be zero. Note that the term that was found proportional to $\sin(\phi_0)\sin(2\phi_0)$ in Eq. (3) is unequivocally confirmed by the measurements in our experimental configuration. In the configuration where $h_{\rm rf}$ is perpendicular to the film plane, $V_{\rm AMR}(H,\phi_0)$ has the same angle dependence of $V_{\rm SP}(H,\phi_0)$, namely $\cos(\phi_0)$, so that one cannot separate the two contributions from the measured angle dependence. Figures 5(a) and 5(b) show the dependence of the total voltage and the parameters $A_{\rm Sym}$ and $B_{\rm Antisym}$, respectively, with the incident microwave power for Py(18.5 nm)/Pt(6 nm) at $\phi_0 \cong 0°$. The measured linear dependence confirms the results predicted by Eqs. (3) and (7).

A crucial test of the theory for the spin-pumping voltage is provided by its comparison to data obtained in samples with varying thicknesses of the FM and NM layers. The symbols in Fig. 6 represent the measured $V_{\rm SP}$ for samples with fixed $t_{\rm Pt} = 10.2$ nm and varying $t_{\rm FM}$. The fast decrease in $V_{\rm SP}$ with decreasing $t_{\rm FM}$ is certainly due to the behavior of the damping parameter produced by the spin-pumping mechanism as well by the effective magnetization decreasing for thin Py layer.[8,25–27] The inset in Fig. 6 shows data for the damping parameter α measured by FMR for fixed $t_{\rm Pt} = 10.2$ nm and varying $t_{\rm FM}$. The solid line in the inset of Fig. 6 is the best fit to the data using $\alpha = \alpha_0 + (\gamma\hbar g^{\uparrow\downarrow}/4\pi M_0 t_{\rm FM})$, according to Ref. 8. From this fit, we obtain, for the spin-mixing conductance $g^{\uparrow\downarrow} = 2.4 \times 10^{15}{\rm cm}^{-2}$, a value similar to that obtained for Pt by other authors,[8,15] and $\alpha_0 = 6.0 \times 10^{-3}$ for the intrinsic damping. The solid line in Fig. 6 is a fit to the $V_{\rm SP}(t_{\rm FM})$ data obtained with Eq. (7) and the parameters given below.

The data for $V_{\rm SP}(t_{\rm Pt})$ obtained with fixed $t_{\rm Py} = 18.5$ nm, shown by the symbols in Fig. 7, are interpreted with Eq. (7) using for the additional damping α'given by Eq. (6) with the following material parameters: $4\pi M_0 = 11.5$ kG, $K_s = 2.0 \times 10^{-3}$ Oe · cm, $\gamma = 1.76 \times 10^7$ (Oe s)$^{-1}$, $g^{\uparrow\downarrow} = 2.4 \times 10^{15}$ cm^{-2}, $\alpha_0 = 6.0 \times 10^{-3}$, $\sigma_{\rm Pt} = 2.42 \times 10^4\ \Omega^{-1}$ cm^{-1} (Ref. 15), and $\varepsilon = 0.1 \approx (\alpha_{\rm fine} \times Z)^4$, where $\alpha_{\rm fine} = 1/137$ and Z is the atomic number of Pt. From the best fit of theory to data shown by the solid line in Fig. 7, we obtain $\lambda_{\rm SD} = 3.7 \pm 0.2$ nm and $\gamma_H = 0.08 \pm 0.01$. Note that the

value for λ_{SD} is similar to that obtained for Pt by other authors.[28] Regarding the spin Hall angle γ_H, there is a wide discrepancy in the values reported in the literature. While the value measured here,$\gamma_H = 0.08 \pm 0.01$, is similar to that reported in Refs. 28 and 29, it is much larger than the one reported in Ref. 15. The authors of Ref. 15 reported a value of $\gamma_H = 0.0067$ and later[20] they refined their result for a value of $\gamma_H = 0.013$. The huge variation reported by this group might be explained by the fact that the symmetric component of V_{AMR} was not properly considered.

In summary, we have shown that the dc voltage generated in FM and NM bilayers under ferromagnetic resonance driven by a microwave field has two components, one due to the AMR and one due to spin pumping from the FM layer into the NM layer. The AMR component has two contributions, one symmetric and one antisymmetric, in field scans relative to the FMR field value, whereas the spin pumping has only a symmetric component. Fit of theory to data of the dc voltage as a function of the in-plane field angle allows an accurate separation of the contributions arising from AMR and from the spin pumping. The data for the dependence of the V_{SP} on the thicknesses of the FM and NM layers are in excellent agreement with theory.

ACKNOWLEDGEMENT

This work was supported by the Brazilian agencies FINEP, CNPq, CAPES, and FACEPE.

*Corresponding author: aac@df.ufpe.br

[1] *Concepts in Spin Electronics,* edited by S. Maekawa (Oxford University, Oxford, 2005).
[2] J. C. Slonczewski, J. Magn. Magn. Mater. **159**, L1 (1996); **195**, L261 (1999).
[3] L. Berger, Phys. Rev. B **54**, 9353 (1996).
[4] S. I. Kiselev, J. C. Sankey, I. N. Krivorotov, N. C. Emley, R. J. Schoelkopf, R. A. Buhrman, and D. C. Ralph, Nature (London) **425**, 308 (2003).
[5] W. H. Rippard, M. R. Pufall, S. Kaka, S. E. Russek, and T. J. Silva, Phys. Rev. Lett. **92**, 027201 (2004); S. Kaka, M. R. Pufall, W. H. Rippard, T. J. Silva, S. E. Russek, and J. A. Katine, **437**, 389 (2005).
[6] S. M. Rezende, F. M. de Aguiar, and A. Azevedo, Phys. Rev. Lett. **94**, 037202 (2005); Phys. Rev. B **73**, 094402 (2006).
[7] A. Slavin and V. Tiberkevich, IEEE Trans. Magn. **45**, 1875 (2009).
[8] Y. Tserkovnyak, A. Brataas, and G. E. W. Bauer, Phys. Rev. Lett. **88**, 117601 (2002); Y. Tserkovnyak, A. Brataas, G. E. W. Bauer, and B. I. Halperin, Rev. Mod. Phys. **77**, 1375 (2005).
[9] A. Brataas, Y. Tserkovnyak, G. E. W. Bauer, and B. I. Halperin, Phys. Rev. B **66**, 060404(R) (2002).
[10] E. Saitoh, M. Ueda, H. Miyajima, and G. Tatara, Appl. Phys. Lett. **88**, 182509 (2006).
[11] A. Azevedo, L. H. Vilela Leão, R. L. Rodriguez-Suarez, A. B. Oliveira, and S. M. Rezende, J. Appl. Phys. **97**, 10C715 (2005).
[12] Y. S. Gui, N. Mecking, X. Zhou, G. Williams, and C.-M. Hu, Phys. Rev. Lett. **98**, 107602 (2007); N. Mecking, Y. S. Gui, and C.-M. Hu, Phys. Rev. B **76**, 224430 (2007).
[13] H. Y. Inoue, K. Harii, K. Ando, K. Sasage, and E. Saitoh, J. Appl. Phys. **102**, 083915 (2007).
[14] K. Ando, Y. Kajiwara, S. Takahashi, S. Maekawa, K. Takemoto, M. Takatsu, and E. Saitoh, Phys. Rev. B **78**, 014413 (2008).
[15] O. Mosendz, J. E. Pearson, F. Y. Fradin, G. E. W. Bauer, S. D. Bader, and A. Hoffmann, Phys. Rev. Lett. **104**, 046601 (2010).
[16] Y. Kajiwara, K. Harii, S. Takahashi, J. Ohe, K. Uchida, M. Mizuguchi, H. Umezawa, K. Kawai, K. Ando, K. Takanashi, S. Maekawa, and E. Saitoh, Nature (London) **464**, 262 (2010).
[17] M. V. Costache, M. Sladkov, S. M. Watts, C. H. van der Wal, and B. J. van Wees, Phys. Rev. Lett. **97**, 216603 (2006).
[18] M. V. Costache, S. M. Watts, C. H. van der Wal, and B. J. van Wees, Phys. Rev. B **78**, 064423 (2008).
[19] X. Wang, G. E. W. Bauer, B. J. van Wees, A. Brataas, and Y. Tserkovnyak, Phys. Rev. Lett. **97**, 216602 (2006).
[20] O. Mosendz, V. Vlaminck, J. E. Pearson, F. Y. Fradin, G. E. W. Bauer, S. D. Bader, and A. Hoffmann, Phys. Rev. B **82**, 214403 (2010).
[21] W. G. Egan and H. J. Juretschke, J. Appl. Phys. **34**, 1477 (1963); W. M. Moller and H. J. Juretschke, Phys. Rev. B **2**, 2651 (1970).
[22] K. Kaski, P. Kuivalainen, and T. Stubb, J. Appl. Phys. **49**, 1595 (1978).
[23] A. G. Gurevich and G.A. Melkov, *Magnetization Oscillations and Waves* (CRC Press, Boca Raton, Florida, 1996).
[24] Y. Guan, W. E. Bailey, E. Vescovo, C.-C. Kao and D. A. Arena, J. Magn. Magn. Mater. **312**, 374 (2007).
[25] B. Heinrich, Y. Tserkovnyak, G. Woltersdorf, A. Brataas, R. Urban, and G. E. W. Bauer, Phys. Rev. Lett. **90**, 187601 (2003).
[26] J. Foros, G. Woltersdorf, B. Heinrich, and A. Brataas, J. Appl. Phys. **97**, 10A714 (2005).
[27] B. Kardasz and B. Heinrich, Phys. Rev. B **81**, 094409 (2010).
[28] K. Ando, S. Takahashi, K. Harii, K. Sasage, J. Ieda, S. Maekawa, and E. Saitoh, Phys. Rev. Lett. **101**, 036601 (2008).
[29] L. Q. Liu, T. Moriyama, D. C. Ralph, and R. A. Buhrman, Phys. Rev. Lett. **106**, 036601 (2011).